

Technology Validation of the Autonomous Formation Flying Sensor for Precision Formation Flying

Jeffrey Y. Tien, George H. Purcell, Luis R. Amaro, Lawrence E. Young, MiMi Aung,
Jeffrey M. Srinivasan, Eric D. Archer, Andrew M Vozoff, Yong Chong
Jet Propulsion Laboratory, California Institute of Technology
4800 Oak Grove Dr, Pasadena, CA. 91109
818-393-1642
Jeffrey.Y.Tien@jpl.nasa.gov

Abstract—A Radio Frequency (RF) based sensor, called the Autonomous Formation Flying (AFF) sensor¹, has been developed to enable deep space precision formation flying by measuring the relative range and bearing angles between multiple spacecraft. The AFF sensor operates at Ka-band and uses signal-processing schemes inherited from the Global Positioning System (GPS). The key features of the AFF sensor are: (a) it operates autonomously without the aid of spacecraft or ground control, (b) it simultaneously provide a wide field of view and accurate range and bearing angle measurements, and (c) it provides accuracy better than 2 cm and 1 arcmin ($1-\sigma$) near the bore-sight of the antenna. In this paper we describe the key technology challenges, the approach to resolving them through analysis and testbed activities, and the results of the testbed activities.

Table of Contents

.....

1. INTRODUCTION
2. KEY FEATURES OF THE AFF SENSOR AND PERFORMANCE REQUIREMENTS
3. AFF SENSOR OVERVIEW
4. KEY TECHNICAL CHALLENGES
5. TECHNOLOGY DEVELOPMENT
6. CONCLUSION
7. FUTURE WORK

ACKNOWLEDGE
REFERENCES

1. INTRODUCTION

The StarLight Mission, an element of NASA's Origins Program, was designed for first-time demonstration of two technologies: optical interferometry between spacecraft and autonomous precise formation flying of an array of spacecraft to support optical interferometry².

These technologies will be applicable to future missions such as the Terrestrial Planet Finder (TPF), Planet Imager, MAXIM, and other missions requiring precise autonomous formation flying to enable a distributed instrument to operate cooperatively across multiple spacecraft. The StarLight mission is composed of two spacecraft, the Collector spacecraft and the Combiner spacecraft (see Figure 1). After initial checkout in an Earth-like heliocentric orbit, the two spacecraft separate and begin flying in formation at separations between 30 and 1000 meters, without real-time intervention from ground-based Mission Operations. Operation of the optical interferometer requires alignment of the relative optical paths to 20-arc-seconds and nano-meter levels of accuracy. This alignment is achieved in multiple steps, starting from a lost-in-space condition. In the first step, a radio frequency (RF) system, the Autonomous Formation Flying (AFF) sensor enables precise formation flying with a control accuracy of ± 10 cm in range and ± 4 arc-minutes in bearing angle. This accuracy is within the search range of the optical metrology system. Optical metrology uses a siderostat (steerable mirrors) to direct light from the Combiner to the Collector, achieving 20-arc-seconds pointing accuracy. Finally, after the detection of the fringes, the delay line within the interferometer stabilizes the optical path delay at the nano-meter level.

In order to enable control at the level specified above, the AFF sensor must supply knowledge at even greater accuracy. StarLight requires the AFF sensor to provide knowledge of spacecraft separation with a maximum uncertainty of 2 cm ($1-\sigma$), and the bearing angles of the remote spacecraft with a maximum uncertainty of 1 arc-minute ($1-\sigma$) in the nominal observing configuration. In addition, to support acquisition and fault recovery, the sensor must operate with reduced accuracy over a wide field of view.

¹ U.S. Patent No. 6,072,433

² In February 2002, the StarLight mission was cancelled by NASA owing to funding unavailability. At that time, portions of the StarLight technology work applicable to the Terrestrial Planet Finder (TPF)

mission, including the Autonomous Formation Flying (AFF) Sensor technology, were adopted by the TPF technology program. In this paper, the AFF Sensor is presented within the StarLight context.

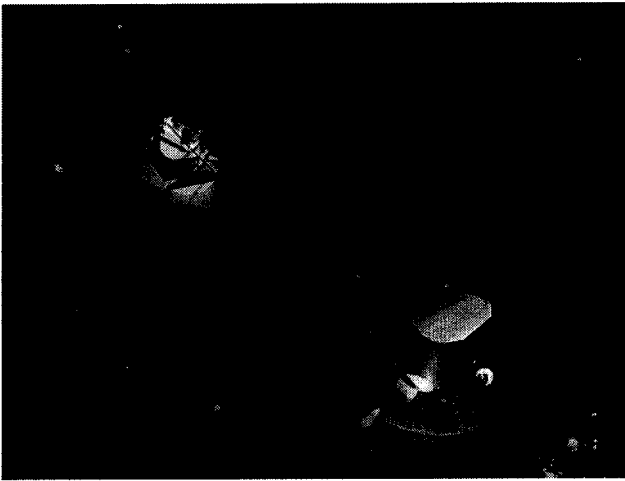


Figure 1 – Preliminary design of the Collector (left) and Combiner (right) spacecrafts for the StarLight Mission.

A significant challenge lies in the simultaneous requirements for high accuracy and a wide field of view mandating a substantial technology development effort and design of a sensor with some novel features. To retire the key technology risks, we developed a prototype Ka-band AFF sensor that allowed us to verify the basic algorithms, validate the complex system distributed over multiple spacecraft, and assess the sensor’s end-to-end performance in the spacecraft structural environment. This paper presents an overview of the design and results of the technology effort

2. Key Features of the AFF Sensor and Performance Requirements

Key Features of the AFF Sensor

The AFF sensor is novel in that it performs all of the following functions:

1. It provides unprecedented accuracy in real-time range and bearing angle measurements: (2 cm, 1 arcmin) 1σ accuracy at spacecraft separations up to 1 km in the “directly facing” configuration defined below.
2. It operates with a nearly $4\text{-}\pi$ -steradian field of view.
3. It operates autonomously:
 - a. No real-time ground-based intervention.
 - b. Self-contained instrument including transmit, receive, and data communication hardware and software on multiple spacecraft.
 - c. Architecture applicable to deep space missions with no reliance on the Earth-based GPS system.
4. It generates estimates of range and bearing angle for use in real-time by the formation flying control system.

Performance Requirements

The purpose of the AFF sensor on StarLight is to provide range and bearing angle measurements between the two spacecraft to enable lost in space recovery, collision avoidance, and precision formation flying in the nominal face-to-face orientation for interferometry. In order to reflect these distinct operating scenarios, Starlight’s requirements on the performance of the AFF sensor are specified for three operating ranges, as shown in Table 1, 2, and 3:

- Operating Range (30–1000 m)
- Close Recovery Range (10–30 m)
- Distant Recovery Range (1000–10,000 m)

Each distance range is further sub-divided into three regions of relative orientation:

- Directly Facing: angle α between lines of sight and normal to front side of spacecraft $\leq 2^\circ$, both spacecraft.
- Nearly facing: $2^\circ < \alpha \leq 45^\circ$ for more miss-pointed spacecraft.
- Not facing: $45^\circ < \alpha$ for more miss-pointed spacecraft.

Table 1. Requirements for AFF sensor performance in Operating Range ($1\text{-}\sigma$).

	Facing	Nearly Facing	Not Facing
Range (cm)	2	2-30	160
Range Rate (mm/s)	1	1	none
Bearing Angle (arcmin)	1	1-600	5400
Bearing Rate (arcsec/sec)	10	20	none

Table 2. Requirements for AFF sensor performance in Close Recovery Range ($1\text{-}\sigma$).

	Facing	Nearly Facing	Not Facing
Range (m)	2	2	3
Range Rate (cm/s)	1	1	none
Bearing Angle (degree)	10	10-15	none
Bearing Rate (arcmin/sec)	10	10	none

Table 3. Requirements for AFF sensor performance in Distant Recovery Range ($1\text{-}\sigma$).

	Facing	Nearly Facing	Not Facing
Range (m)	2	2	none
Range Rate (cm/s)	none	none	none
Bearing Angle (degree)	10	10-15	none
Bearing Rate (arcmin/sec)	none	none	none

The most stringent requirements are the 2-cm range and 1-arc-minute bearing-angle requirements when the spacecraft are directly facing each other in the operating range during the interferometric observation mode. These challenging requirements are the key drivers for most of the technology development work on the AFF sensor.

3. AFF Sensor Overview

AFF Sensor Design

The AFF sensor is a distributed RF sensor that operates at Ka-band. It is a self-contained system with transmitters and receivers for both radiometric and data transfer on both spacecraft. It consists of virtually identical hardware and software on each spacecraft. The baseline AFF sensor configuration for StarLight is 2 transmitting antennas and 4 receiving antennas on each spacecraft:

- 1 transmitting antenna and 3 receiving antennas on the facing or front side, and
- 1 transmitting antenna and 1 receiving antenna on the backside.

The antennas on the facing side allow full estimation of range and bearing angle, while the antennas on the back assist the spacecraft in finding each other in the event they get turned around. This configuration gives near-global coverage.

The two halves of the sensor transmit to and receive from the other spacecraft in full duplex. The signal structure is similar to that used by the GPS:

$$S(t) = P(t) D(t) \text{Cos}(2\pi ft + \phi)$$

where

$P(t)$ = ranging code

$D(t)$ = telemetry modulation

f = Ka-band carrier frequency

ϕ = carrier phase due to range, clock offsets, etc.

The key observables for the AFF sensor are pseudorange, which is derived from tracking the ranging codes, and carrier phase. The range between the two spacecraft is determined mainly from the pseudorange measurements, whereas the bearing angles (azimuth, elevation) are derived mainly from the carrier phase measurements differenced between receiving antennas. During operation, independent range and bearing angle solutions are estimated simultaneously on each spacecraft using observables from both spacecrafts. The data are exchanged across the sensor's RF link.

Building Blocks of the AFF Sensor

As shown in Figure 2, the AFF sensor is composed of Ka-band antennas, Ka-band transmitters and receivers, frequency and timing subsystems, and digital baseband processors. The sensor design and performance interact strongly with the spacecraft and interferometer designs. They are inter-dependent in terms of accommodation, fields –of view, stray light, radio frequency interference, thermal stability, and mechanical stability.

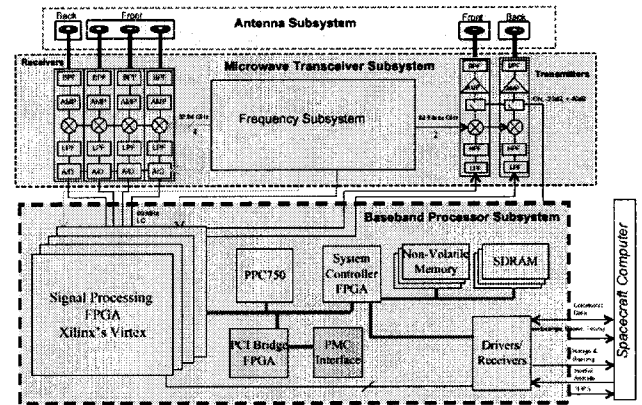


Figure 2. AFF sensor subsystems block diagram.

4. Key Technical Challenges and Mitigation Approach

The key technical challenges for the AFF sensor in meeting the tight performance requirements while operating with a wide field of view in an autonomous environment include:

- Mitigation of multipath
- Calibration of time-varying instrumental biases
- Implementation of continuous transmission and reception
- Reduction of stochastic ranging errors
- Realization of basic end to end functionality

The mitigation approach for each of the technical challenges is as follows:

- (1) Multipath mitigation:
 - Narrow the antennas' field of view
 - Measure the antenna patterns, including the effect of the spacecraft (build physical models)
 - Model the antenna patterns for in-orbit calibration
- (2) Time-varying instrumental biases:
 - Stabilize the sensor's temperature
 - Measure the sensitivity of range and phase observables to the temperatures of the components
 - Directly measure instrumental phase and delay in situ and calibrate the observables accordingly
- (3) Continuous transmission/reception:
 - Control isolation (time-division duplexing)
- (4) Stochastic ranging errors:
 - Smooth ranges with carrier-aiding
- (5) Basic end-to-end functionality:
 - Develop prototype hardware
 - Develop needed algorithms

- Perform end to end functional test

To validate this design approach to mitigating technical risks, we developed and evaluated a prototype AFF sensor in multiple testbeds:

- (1) Outdoor antenna isolation testbed
- (2) 60 ft anechoic testbed
- (3) Indoor prototype AFF sensor testbed
- (4) 1200-ft outdoor radiating testbed

Figure 3 shows the prototype AFF sensor hardware.

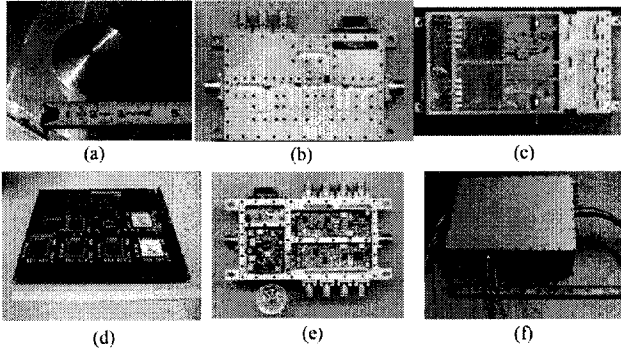


Figure 3. Prototype AFF sensor hardware: (a) Ka-band antenna, (b) Ka-band transmitter, (c) Frequency Synthesizer Module, (d) Baseband Processor, (e) Ka-band Receiver, and (f) Reference Module.

The AFF sensor technology mitigation and validation approach is summarized below in Table 2.

Table 2. AFF Sensor Technology Development Summary Table.

Technical Challenges	Mitigation Approach	Validation Approach
(1) Multipath mitigation -	Narrow antennas' field of view	Anechoic Chamber Testbed
	Measure antenna patterns including the effect of the spacecraft (build physical models)	Anechoic Chamber
	Model the antenna patterns for in-orbit calibration	Anechoic Chamber
(2) Time-varying instrumental biases	Stabilize the temperature of the environment continuous self-calibration scheme	Spacecraft Control Indoor Prototype Testbed
(3) Continuous transmission/reception	Control isolation (time-division duplexing)	Antenna Isolation Testbed
(4) Stochastic ranging errors	Smooth ranges with carrier-aiding	Indoor Prototype Testbed
(5) Basic end to end functionality	Prototype hardware development	Indoor Prototype Testbed
	Algorithm development	Indoor Prototype Testbed
	Perform end to end functional test	Outdoor Radiated Testbed

A comprehensive error budget analysis was performed, and results from the testbeds were evaluated against the error budget allocations. The descriptions of the testbeds, results and a summary of the technology assessment are presented in the following sections.

5. Technology Development and Results

Antenna Isolation and Multipath

For the StarLight mission, a large sunshade is necessary on each spacecraft as shown in Figure 4 to protect the instrumental instrument from stray light and overheat from the sun. However, for a RF sensor, the sunshade and other spacecraft structure surrounding the antennas modifies the effective pattern of the antenna because of multipath and diffraction effects. Two major concerns for the sensor performance are: (1) the isolation between the transmitting antennas and the receiving antennas; and (2) deviation of the actual antenna patterns on the spacecraft from the nominal patterns in isolation.

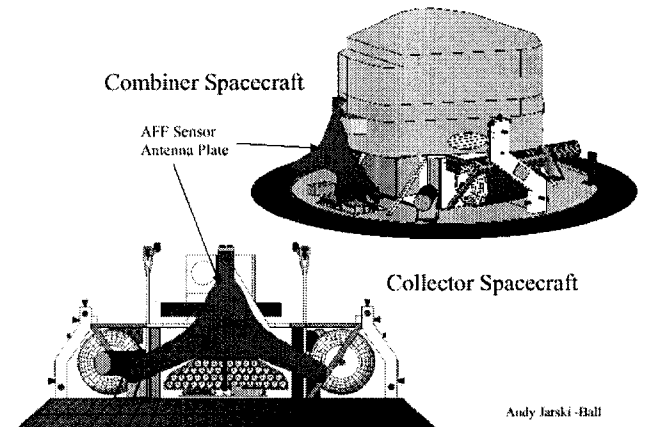


Figure 4. StarLight Spacecrafts.

The performance of the Ka-band antennas within the StarLight spacecraft structural environment was evaluated in the following antenna testbeds. The antennas were prototyped and physical models of the antenna mounting plate and the spacecraft sunshades (for both the Combiner and the Collector spacecraft) were constructed. Then the performance of each antenna was assessed within the structurally modeled environment.

Antenna Isolation Testbed

According to the current baseline design for StarLight, the AFF sensors on both the Combiner and the Collector spacecraft will transmit and receive simultaneously and continuously. Because of the short distance (~0.5 meter) between the transmitting antenna and the receiving antennas on the mounting plate, special effort needs to be applied to reduce the signal leaked from the transmitting antenna to any receiving antenna to a level well below the noise power generated by the receivers' front-end electronics. This control prevents the leakage signal from jamming the receiving channels. In addition, the delay of

the leakage signal needs to be stable enough to allow its use for phase and group-delay calibration.

If the available means fail to provide enough isolation between the transmitting antennas and the receiving antennas, or if the leakage signal is not stable enough for group delay and phase delay calibration, then Time Division Duplexing (TDD) will need to be implemented on the AFF sensor.

To evaluate the isolation between the transmitting and receiving antennas, the antennas and the structural models were set up as shown in Figures 5 and 6. The transmitting antenna and the adjacent receiving antennas were pointed towards the sky. While the transmitting antenna transmitted, the signals received at the receiving antennas were measured. The isolation of each receiving antenna was defined as the ratio of the received signal power to the transmitted power. Measurements were made with and without the sunshade mockups attached.

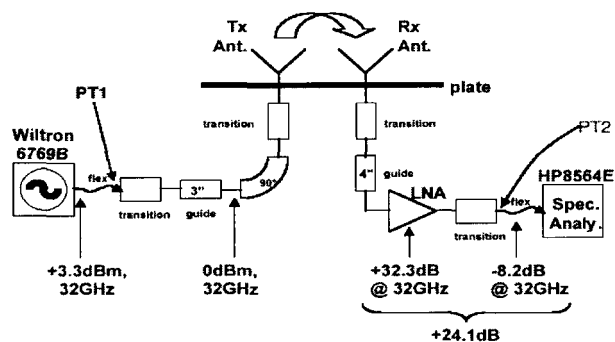
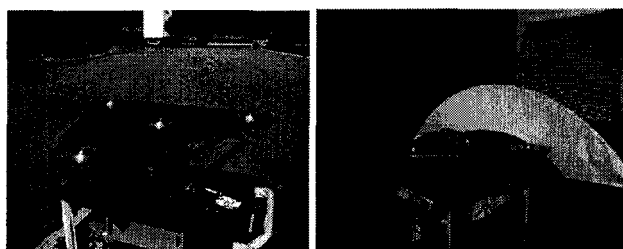


Figure 5. Antenna isolation test setup.



Without Sunshade With Combiner Sunshade

Figure 6. Antenna Isolation Testbed.

The significant results are:

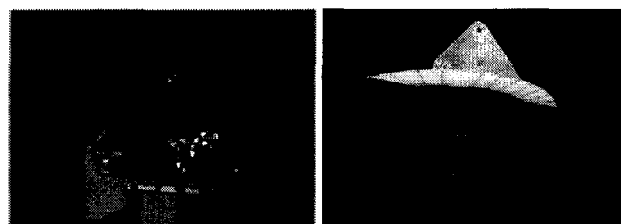
1. The measured isolation matches exactly the space loss predicted by Friis's equation. This is a significant, positive result that indicates that there are no significant surface effects on the mounting plate. This conclusion is further supported by the fact that the isolation level remained virtually unchanged when the plate was removed and when multi-layer insulation (MLI) was laid on the plate. Insensitivity to MLI is desirable, as MLI may be necessary for thermal control.

2. The isolation between the transmitting and receiving antennas was degraded by the multipath and diffraction effects of the sunshades. The degradation depended directly on the shape of the sunshade. With the Combiner sunshade, the range extended from -80 dB to -73 dB. With the Collector sunshade, which has the sharper slope away from the antennas, isolation ranged between -86 dB and -80 dB). The sharper the angle of the sunshade away from the antennas, the smaller was the degradation of the isolation.
3. Repeatability of the isolation levels when there is variation in the separation between the antennas and the sunshades was poor. This result is due to the fact that the uncertainty in mechanical positioning is non-negligible relative to the short wavelength at Ka-band. This fact must be taken into account when considering using the transmitted leakage signal as a part of the self-calibration scheme, as biases can be introduced easily by pre- and post-launch shifts in the sunshade and by thermal variations. Both the instability and the inadequacy of the natural leakage path favor a TDD calibration scheme, with a controlled fixed-amplitude signal on a stable internal path.

60-Foot Anechoic Testbed

Multipath is the dominant source of error for the AFF sensor and was also the error source with the biggest uncertainty. For the StarLight mission, a large sunshade is necessary on each spacecraft to protect the instrumental instrument from stray light and solar heating. However, for a RF sensor, the sunshade is the primary source of multipath.

To evaluate the effect of the multipath and diffraction on the antenna pattern, tests were set up in an anechoic chamber as shown in Figure 7. The transmitting and receiving antennas were mounted on the mockup of the mounting plate, and patterns were cut with and without the sunshade mockups attached. A pair of antenna gain patterns and phase patterns, the first without the sunshade and the other with a sunshade, is shown in Figure 8 and Figure 9 respectively. These results show that the antenna gain patterns' contributions to the range and the antenna phase patterns' contributions to the bearing errors are not negligible.



Without Sunshade With Combiner Sunshade

Figure 7. 60 ft Anechoic Chamber Testbed.

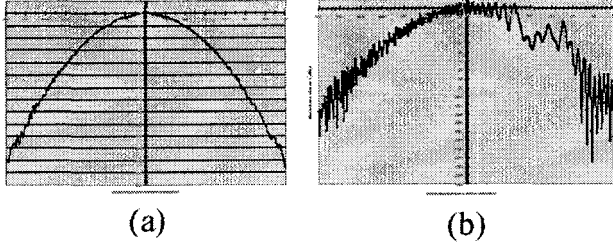


Figure 8. (a) Antenna gain pattern without the sunshade, (b) lower antenna gain pattern with Combiner sunshade.

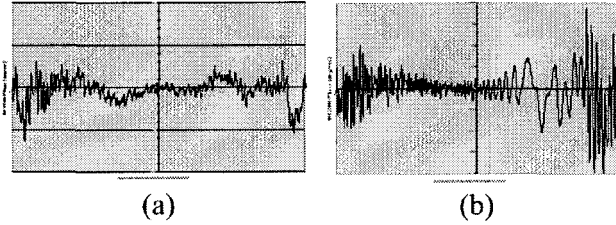


Figure 9. (a) Antenna phase pattern without the sunshade, (b) lower antenna phase pattern with Combiner sunshade.

To evaluate the impact of the antenna pattern deviations on the sensor's performance, the worst-case deviation from the ideal pattern was measured and its contribution to the error in estimation of the range and bearing angle estimates was evaluated.

The assumptions for the error contributions are as follows:

- Relative gains of the transmitting and receiving antennas at the specified beam angle
 - Affects system noise error
 - Assumed configuration has the two s/c pointed in opposite directions in inertial space, range vector offset in the y-z ("horizontal") plane by the tabulated amount
- Contributions to un-calibrated phase and range error from both the specified receiver and the transmitter on the other spacecraft.
- For range, a realistic estimate of the excess multipath delay for each antenna
 - Range from 6 cm for a lower antenna to 75 cm for an upper antenna
 - Reflection point assumed at rim of sun shade directly in front of the antenna

The error contribution was compared to the error budget allocation. The results as shown in Table 3 showed that within the overall error budget, the deviations due to multipath and diffraction effects are well within the error allocation. In the "directly facing" configuration, the sensor can meet the (2 cm, 1 arcmin) requirement in range and bearing angle estimation. In the "nearly-facing" and "not facing configurations", the deviations still satisfy the looser requirements for those regions. This shows that the

performance requirements can be met in the StarLight configuration.

Table 3. Estimated Parameter Errors (1σ).

Parameter	Calculated Uncertainty / Requirement			
	0° - 2°	5°	45°	70°
Range (cm)	0.564 / 2	0.616 / 2	2.216 / 30	5.870 / 160
Bearing Angle ("azimuth") (arcmin)	0.976 / 5	1.002 / 5	3.257 / 600	17.43 / 5400
Bearing Angle ("elevation") (arcmin)	0.872 / 5	0.879 / 5	2.147 / 600	5.36 / 5400

Prototype AFF Sensor Indoor Testbed

To verify the basic algorithms and calibration schemes in a multiple-spacecraft environment, a prototype sensor testbed was developed. The testbed is shown in Figure 10. It is composed of two halves, each side representing a spacecraft. Each spacecraft consists of the Ka-band modules, frequency synthesizers, and a digital baseband processor. The waveguides and attenuators connecting the two halves represent the space loss. Microwave assemblies are thermally controlled for studies involving thermal variations. This prototype is fully operational. The test results are discussed below.

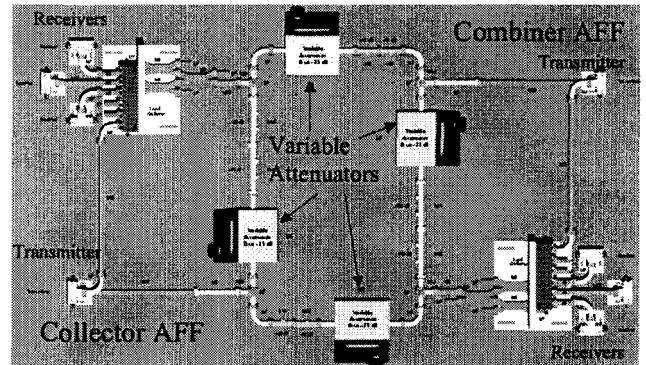


Figure 10. Prototype AFF sensor indoor test setup.

Continuous Self-Calibration Scheme

Estimation requirements for range (2 cm) and bearing angles (1 arcmin) demand extreme stability from the AFF RF electronics:

- Instrumental delay: $(2 \text{ cm}/c) = 67 \text{ ps}$
- Differenced instrumental phase: $(2.909 \times 10^{-4} \times 1 \text{ m})/\lambda_{\text{rf}} = 0.032 \text{ cycle} = 0.98 \text{ ps}$.

The required stability probably is not attainable directly, particularly for the delay observable. A scheme is therefore needed to monitor instrumental delay and phase continuously and compensate the observable accordingly. For this purpose, a continuous self-calibration scheme has been designed to remove the effect of instrumental variations on the delay and phase observable. This is accomplished by having the receiver tracking both the remote signal from the other spacecraft and its own transmitting signal simultaneously to remove the instrumental variations.

This scheme has been verified on the prototype system. Results of self-calibration on the phase observable and the range observable are shown in Figure 11 and Figure 12 respectively.

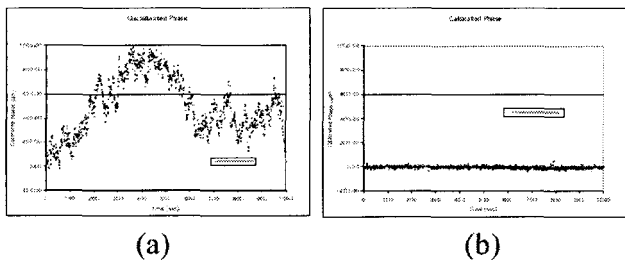


Figure 11. (a) Un-calibrated phase measurement, (b) Calibrated phase measurement.

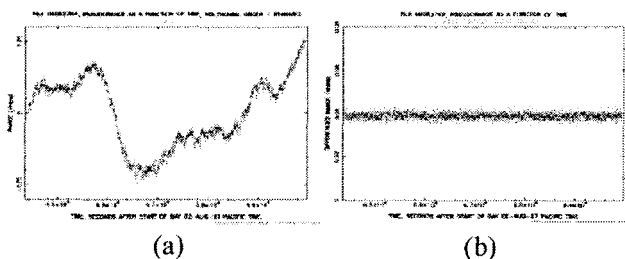


Figure 12. (a) Un-calibrated range measurement, (b) Calibrated range measurement.

It is clear from the results that the instrumental variation on the phase and range observables is removed by the full calibration technique.

Carrier-aided Range Estimation

Without carrier-aided smoothing of the group delay, the system noise would likely be the dominant error source for the range measurement, and it might prevent the AFF sensor from meeting the 2-cm range accuracy requirement.

The approach to mitigating this risk is to use carrier-aided smoothing to reduce the group delay system noise. This technique exploits the fact that the AFF phase observable provides very accurate values of range rate. It is used routinely in the analysis of GPS measurements, but its applicability to the AFF sensor needs to be validated to show that the coherence of the sensor's calibrated range and phase observable are adequate. Our results, shown in Figure 13, show that the AFF sensor can indeed support this algorithm. Figure 13(a) shows the range observable before carrier-aided smoothing, and Figure 13(b) shows the observable after 100 seconds of smoothing. The standard deviation about the observable is reduced by the expected ratio, $1/\sqrt{n}$, where n is the number of points over which the range observable is smoothed.

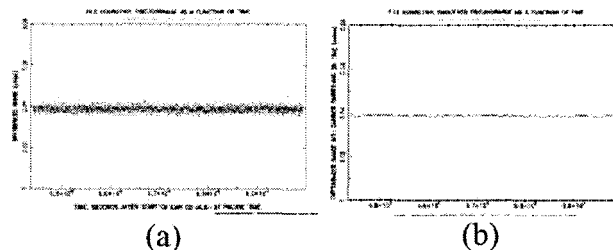


Figure 13. (a) Range measurement before smoothing, (b) Range measurement after smoothed by carrier phase for 100 sec.

Outdoor 1200 feet Radiated Testbed

The objectives of the outdoor radiated test are to demonstrate:

1. End to end AFF sensor functionality.
2. Range change measurements.
3. Bearing change measurements
4. Absolute range measurements

The purpose of this test is to verify end-to-end AFF sensor functionalities. The performance results is expected to be worse than the flight environment given the multipath environment surrounding the test setup.

The test is conducted across the JPL Mesa 1200 feet antenna test range as shown in Figure 14 with AFF sensor mounted on the east side representing the AFF sensor on one spacecraft and AFF sensor mounted on the west side representing the AFF sensor on the other spacecraft.

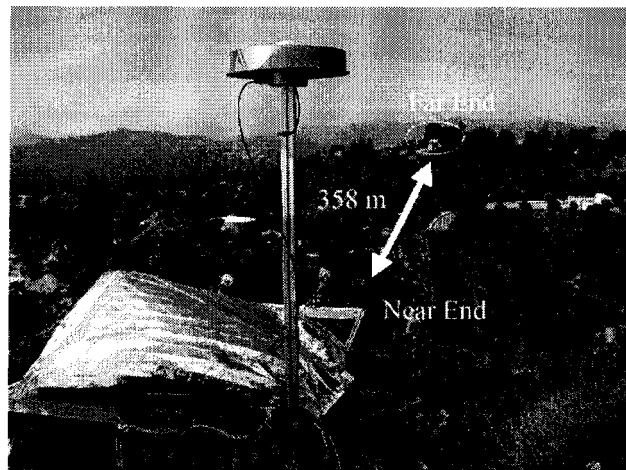
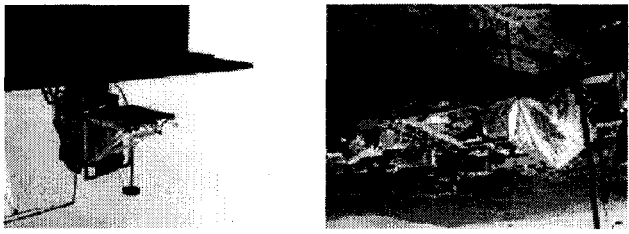


Figure 14. JPL Mesa 1200 feet antenna test range.

The east side AFF sensor is consisting of one transmitter and one receiver mounted on a sliding rail as shown in Figure 15 (a). The west side AFF sensor is consisting of one transmitter and two receivers mounted on a rotating pedestal as shown in Figure 15(b). The separating distance between the two receiving antenna on the west side is one meter.

Figure 15. (a) East side AFF sensor, (b) West side AFF sensor.



TurboRogue GPS receiver is used to serve as the absolute truth sensor for the range measurement with accuracy of better than 1 cm. A MTS Tempsonics Transducer is used to provide range change measurement with resolution of 0.1 mm. For the bearing angle, the west-side rotating pedestal provides a angular resolution of 0.02 degree.

The test results shows that the end-to-end AFF sensor functionality has been successfully verified. Figure 16 shows the results of the measurement of range change using phase data. The slide rail on the east side test setup was moving in 3 mm steps while the west side test setup was in a fixed position.

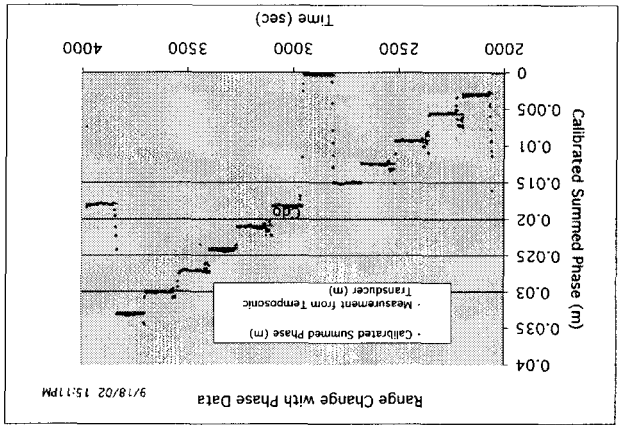


Figure 17 shows the bearing angle measurement with the west side test setup rotating both direction in 5 degree steps while the east side test setup is in a fixed position.

Figure 16. Range change measurement using phase data.

Figure 17. Bearing angle measurement using differenced phase data.

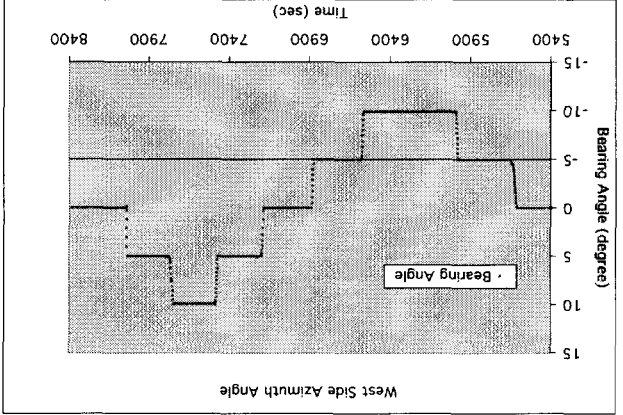


Figure 18 shows the static bearing angle measurement with better than 0.3 arcmin precision.

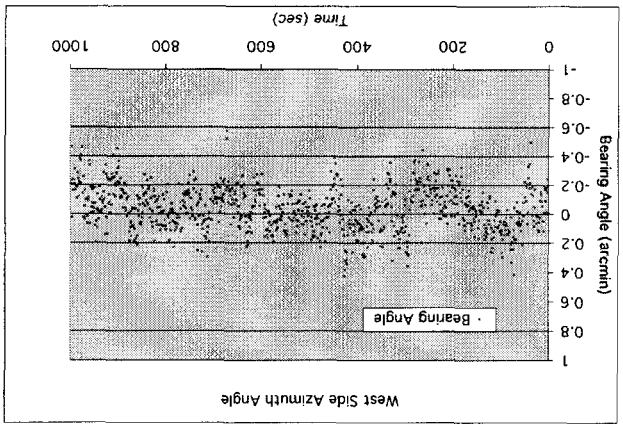


Figure 18. Bearing angle precision.

AFF sensor end to end functionality has been successfully verified in the JPL Mesa 1200 feet antenna test range.

Summary of the Technology Results

AFF sensor evaluation tests have been performed in three areas. The antenna testbeds (Figures 6 and 7) were used to verify the RF antenna performance, while the AFF Sensor prototype testbed (Figure 10) was used to verify the sensor architecture and the algorithm performance. The end-to-end functionality test completes the full assessment of the sensor. Through these tests, many of the technical concerns have been understood and retired, while other concerns provided insight leading to modification of the baseline design.

- The concerns which have been retired at this time are:
- (1) effectiveness of the algorithms for self-calibration,
 - (2) effectiveness of carrier-aided smoothing of the range observable;
 - (3) ability to measure the antenna patterns and account adequately for multipath and diffraction;
 - (4) operability of the complex Ka-band scheme.

One concern that led to modification of the baseline design was the level of isolation between the transmitting and receiving antennas in the presence of multipath and diffraction effects. Insufficient and unstable isolation made the external calibration path an unattractive option. Instead the design team chose a stable, manageable internal calibration path along with TDD) to assure reliable calibration and prevent self-jamming. The TDD scheme has been verified to work within the AFF Sensor scheme by tests in the prototype testbed.

6. Summary and Conclusion

The architecture and fundamental algorithms of the AFF sensor have been assessed. The leading technical challenges have been addressed through development of a prototype AFF sensor and tests in multiple testbeds to evaluate performance and verify end-to-end functionality. The results show that the sensor will work with the required performance of (2cm, 1 armin) 1σ accuracy in range and bearing angle estimates within the environment of the StarLight mission.

These results could apply directly to the TPF mission. For TPF and other precision formation flying missions, it is evident that formation-flying sensor performance must be optimized through trade-offs involving the design of the sensor, the spacecraft, and the science instruments. Within the precision formation flying system, performance must be optimized by trading off sensor performance, sensor field of view, spacecraft maneuvers required for acquisition and calibration, and formation control architecture.

7. Future Work

The AFF Sensor will be further assessed for integration into the TPF precision formation flying system. In particular, the following technical assessments need to be made for the TPF spacecraft configuration (Figure 19): multipath and diffraction effects, acquisition techniques, calibration techniques, hand-off to a finer sensor with a narrower field of view, and trade-offs involving sensor performance, field of view, formation flying control design, spacecraft design and the interferometer design.

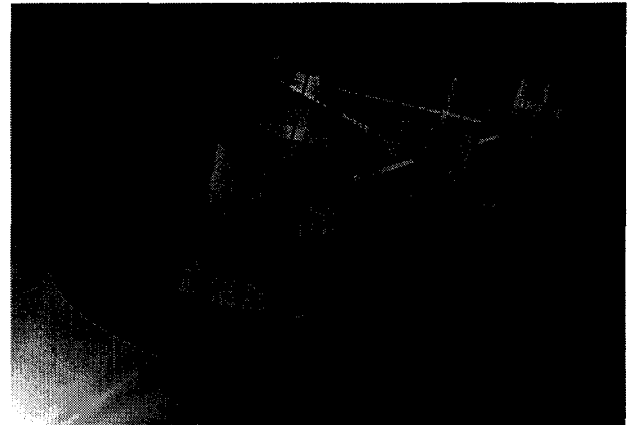


Figure 19. Formation Flying Interferometer (FFI) version of the TPF mission.

Another set of future work is to investigate technologies to integrate high-bandwidth inter-spacecraft communications with the AFF sensor. This concept is motivated by the fact that the sensor already provides an inter-spacecraft link with best performance in the “directly facing” configuration. For the interferometer, the highest data bandwidth requirement is required in the “directly facing” configuration to enable high-speed control loops for the siderostat control system.

Acquisition of Spacecraft Formation

The control system requires the AFF sensor to have widest field of view possible in order to minimize the search time for acquisition. A trade-off has to be performed between the field of view (which involves the antennas and the sunshade design), the control system design, and the associated spacecraft maneuvers.

Currently, a $\pm 70^\circ$ field of view antenna has been designed and assessed for RF performance. Further iterations of the trade between field of view and performance are anticipated in the mission design stage.

Synchronization of the Distributed System

The distributed nature of the sensor on two spacecraft poses challenges in terms of time synchronization, fault-protections, and recovery from a temporary failure of one or both halves. Given that the sensor supports an optical interferometer, its design demands maximum robustness and minimum maintenance. Further work is required in this area.

Acknowledgements

The authors would like to thank Andy Jarski of Ball Aerospace & Technologies Corp., Boulder, Colorado, for supplying the information needed to design the spacecraft mockups. We also thank Phil Mayer, Randy Bartman, Hamid Javadi, and Jacob Gorelik for their valuable

assistance in the design and assembly of the 1200-ft outdoor radiating testbed and the indoor prototype AFF sensor testbed.

The research described here was carried out at the Jet Propulsion Laboratory, California Institute of Technology, under a contract with the National Aeronautics and Space Administration. References herein to any specific commercial product, process or service by trademark, manufacturer, or otherwise, does not constitute or imply its endorsement by the United States Government or the Jet Propulsion Laboratory, California Institute of Technology.

References

G. Purcell, D. Kuang, S. Lichten, S. Wu, L. Young, B. Haines, "Autonomous Formation Flyer (AFF) Sensor Technology Development," American Astronautical Society paper AAS 98-062, 21st Annual AAS Guidance and Control Conference, Breckenridge, CO, February 1998.

J.B. Thomas, "Signal-Processing Theory for the TurboRogue Receiver," Jet Propulsion Laboratory Technical Publication 95-6.

K. Lau, S. Lichten, L. Young, B. Haines, "An Innovative Deep Space Application of GPS Technology for Formation Flying Spacecraft," American Institute of Aeronautics and Astronautics paper AIAA 96-3819, Guidance, Navigation and Control Conference Proceedings, San Diego, CA, July 1996.

L. Young, S. Lichten, J. Tien, C. Dunn, B. Haines, K. Lau, U.S. Patent No. 6,072,433, "An autonomous formation flying sensor for precise autonomous determination and control of the relative position and attitude for a formation of moving objects," June 6, 2000.

M.Aung, G. Purcell, J. Tien, L. Young, L. Amaro, J. Srinivasan, M. Ciminera, Y. Chong. "Autonomous Formation Flying Sensor for the StarLight Mission," International Symposium on Formation Flying Missions & Technologies, Toulouse, France, October, 2002.

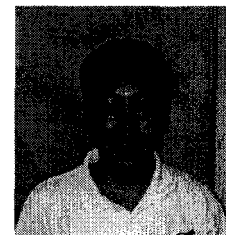
George Purcell, "Progress in Passing Through The AFF 'Carrier-Aided Smoothing' Technology Gate," JPL internal memorandum August 7, 2002.

George Purcell, "Progress in Passing Through the AFF 'Continuous Calibration' Technology Gate," JPL internal memorandum, July 30, 2002.

George Purcell, "Final Steps in Negotiating the StarLight AFF Continuous Calibration and Carrier-Aided Smoothing Technology Gates," JPL internal memorandum, July 30, 2002.

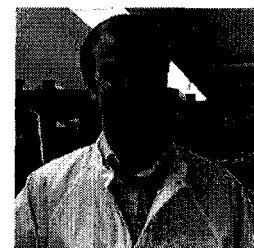
Biography

Jeffrey Tien received his M.S. degree in Electrical Engineering from USC in 1993. He joined the GPS systems group at JPL in 1989 where he worked on hardware design of flight GPS receivers for various space missions. He has served as the Instrument Lead Engineer for the Autonomous Formation Flying sensor on the StarLight Mission for the last two years. His research interest includes high speed signal processing and formation flying sensor technology development



George Purcell has been a member of the Technical Staff at the Jet Propulsion Laboratory since 1975. His research interests and experience include radio interferometry and its geodetic applications, GPS applications, experimental design, and data analysis. Since 1998 he has been working on the development of formation flying technology for StarLight and its predecessors.

Dr. Larry E. Young has developed radiometric technology at Caltech's Jet Propulsion Laboratory since 1978. Specific areas of his group's research include digital GPS receivers, multipath mitigation, sub-nanosecond clock synchronization, and sub-cm formation flying. Larry received a Ph.D. in Nuclear Physics from SUNY at Stony Brook in 1975, and a B.A. in Physics from Johns Hopkins in 1970. He has served on several committees defining future navigation systems, and has been author or co-author of 30 refereed papers, 51 conference proceedings, 10 NASA tech briefs, and 3 GPS-related patents.



Luis R. Amaro. Received his MSEE degree from Cal. State University, Northridge in May of 1998, and his BSEE from Cal Poly, Pomona in 1984. Prior to coming to JPL he worked at Rockwell Intl., and TRW Inc. He has served as Chairman of the I&M Society of the IEEE, Los Angeles Chapter. Since 1991 he has been with the Spacecraft Antennas Group, Spacecraft Telecommunication Section of the Jet Propulsion Laboratory where is a Senior Antenna Engineer. While at JPL he has designed various microwave and millimeter wave components. Mr. Amaro's interests include electromagnetic simulation and the numerical analysis of antennas and micro/millimeter wave components.

MiMi Aung received her M.S. in Electrical Engineering from University of Illinois, Urbana-Champaign in 1990.

She joined JPL in 1990, in the Block V Receiver signal processing team, starting from digital signal processing area, following through into the implementation phase. Next, she led a design team to design a precision pointing of 34-meter beam-waveguide antennas using Monopulse technique, which has subsequently been implemented and made operational by the current Monopulse team led by Wendy Hodgkin. She has been a project element manager in the Network Simplification Project (NSP), from the Downlink Consolidation aspect. Since 2000, she has been the project element manager for AFF Sensor in the StarLight project. Currently, she is the acting project element manager for Formation Flying Technology under Terrestrial Planet Finder pre-project technology program.

Max Vozoff earned his BEE degree from Curtin University, Western Australia in 1993 and is currently completing his MSAE at USC. He worked as an RF Design Engineer for ERG Telecommunications in Australia designing hardware for Paging Transmitters. In 1998 he moved to Santa Barbara to design ISM-band wireless modems & transceivers for Utilicom Inc. (now Wi-LAN). He joined the Tracking Systems & Applications Section at JPL in 2000, where he works with RF hardware for space flight applications.